JACS
JOURNAL OF THE AMERICAN CHEMICAL SOCIETY
pubs.acs.org/JACS
Article

Torsional Tunneling Splitting in a Water Trimer

Yu-Cheng Zhu,[∇ Y.-C.Z. and S.Y.] Shuo Yang,[∇ Y.-C.Z. and S.Y.] Jia-Xi Zeng, Wei Fang, Ling Jiang, Dong H. Zhang,* and Xin-Zheng Li*

Cite This: J. Am. Chem. Soc. 2022, 144, 21356−21362

ABSTRACT: Using a full-dimensional quantum method for nuclei and a new first-principles water potential, we show that the torsional tunneling splitting in a water trimer can be reproduced with accuracy up to ∼1 cm^{-1}. We quantify the coupling constants of the nuclear quantum states between nonadjacent wells and show that they are the main reason for shifting the quartet-split levels in spectra from a 1:2:1 spacing. This demonstrates the limitation of treatments using simplified models such as the Hückel model and emphasizes the nonlocal nature of the quantum interactions in this system. With such an *ab initio* endeavor, we examine the quality of the water potential developed and provide a rigorous scheme to decipher the experimental spectra with unprecedented accuracy, which is applicable to more general systems.

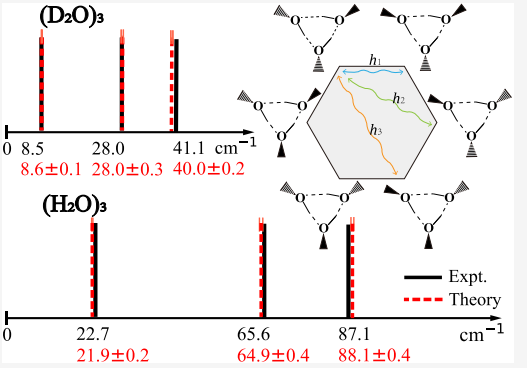

INTRODUCTION

An accurate description of intra- and intermolecular forces of water, represented as a predictive universal water potential energy surface (PES), has long been pursued.[1,2] With the advances of *ab initio* methods, potentials constructed by the many-body expansion (MBE) method have been able to qualitatively predict many features of aqueous systems.[3−6] Among the various experimental criteria in testing the quality of this potential, spectroscopy presents the most challenging one due to the high sensitivity of the spectrum to the quality of the PES and technical difficulties in describing the spectra at the quantum mechanical level.[7] Taking the vibration−rotation−tunneling (VRT) spectrum of water clusters as an example, it provides fine information that is accurate at the order of MHz to kHz.[8−14] It has long been expected to thoroughly explore such experimental data so that highly accurate many-body terms of the water potential can be constructed and a scheme toward systematically improvable one can be achieved.[1,2,7,15,16] However, except for a dimer where a full-dimensional wave function method is applicable,[17] quantum simulations of these spectra in other clusters are still absent due to the curse of dimensionality.

A crucial step along this route resides in a rigorous theory for calculating the tunneling splitting of a water trimer. In this trimer, the facile flip (or torsional) motion of free hydrogen atoms, which can result in a torsional tunneling splitting of ground vibrational levels, is unique.[14] The system transfers between different states through a very low barrier (ca. 10 meV,[18] as no hydrogen bond breaks) and thus presents large splitting sizes up to tens of cm^{-1}. This energy is even comparable to the magnitude of intermolecular vibrations, i.e., translation and libration.[19] They are thousands of times larger than the rotational constants and bifurcation splittings[20,21] (another kind of tunneling splitting proposed in a water trimer involving breaking and reforming of hydrogen bonds) and thus appear as bands containing rotational sublevels in spectra, termed as torsional bands.[8] Here, the traditional perturbative treatments fail because the system would not be trapped in a well, e.g., different wells are visited via the tunneling process, and a strong delocalization of the nuclear wave packet exists. Six degenerate wells (configurations with two of the free hydrogen atoms "up" or "down" the oxygen plane) on an internal potential surface (IPS) are connected as a ring, prompting a pseudorotation motion on cyclic potential[22] (in Figure 1a,b). As such, the interpretation of these splitting levels demands a nonperturbative solution to the nuclear degrees of freedom on IPS quantum mechanically.

At the earliest, a one-dimensional (1-D) model in which six barriers were connected to constitute a periodic potential was constructed.[22] Later, van der Avoird et al. proposed a 3-D internal-rotation Hamiltonian to include respective flips of the three free hydrogen atoms and the rotational coupling.[23] A higher-dimensional description of IPS can yield a more reliable estimation of the splitting size. Therefore, a 4-D treatment was soon employed to further include the symmetric hydrogen-bond stretch mode.[24] However, this is still far from the target

Received: September 16, 2022
Published: November 9, 2022

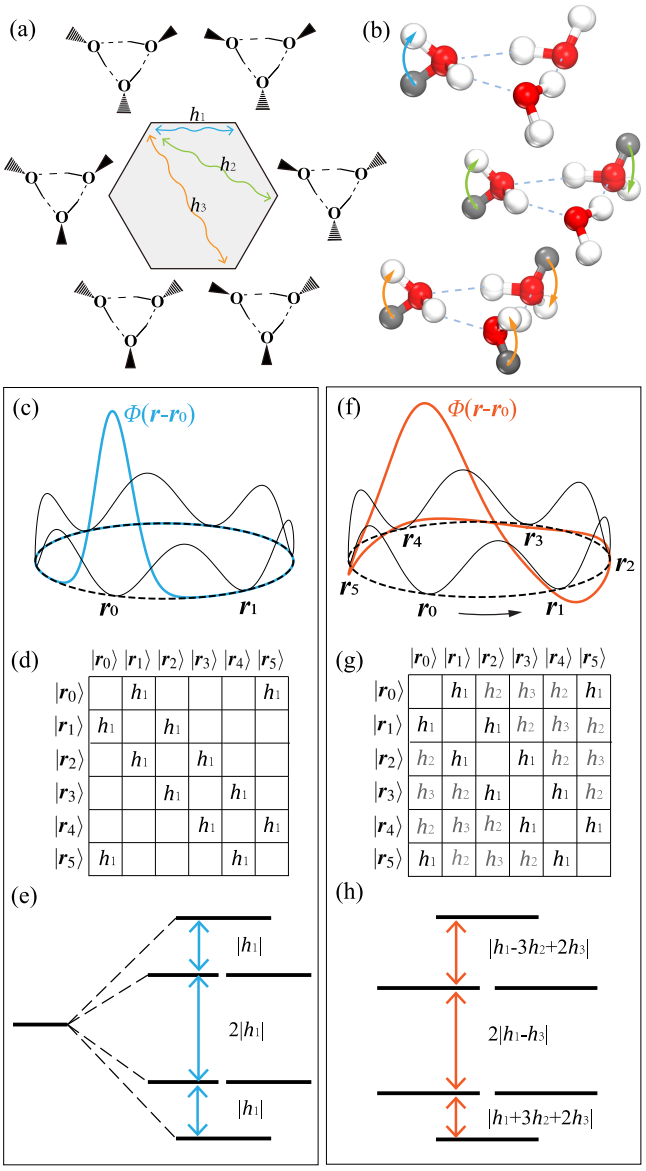

Figure 1. (a) Six wells in the water trimer. h_1, h_2, h_3 are the interactions between 1st, 2rd, and 3rd NN, as shown in (b). The gray and white balls represent the start and end positions of the free hydrogen atoms, respectively. As a schematic, $\phi(\boldsymbol{r} - \boldsymbol{r}_i)$ in (c) and (f) is the Wannier function solved on a 1D model potential with different barrier heights. When barriers are low, strong delocalization manifests as a nonzero amplitude in other wells, as shown in (f). (d) and (g) are the corresponding Hamiltonian matrix, and (e) and (h) show the splitting levels. The inclusion of nonadjacent terms, h_2 and h_3, results in the levels' shifting from a 1:2:1 spacing.

of quantitatively rigorously examining the water potentials,[25] unless a full-dimensional wave function can be solved. The diffusion Monte Carlo (DMC) method[26] may have a chance to realize a full-dimensional calculation but suffers from the required fixed-node approximation for high-level states.[16]

The lowest four eigenstates of the torsional (or internal) Hamiltonian, with 1, 2, 2, and 1 degeneracy, corresponded to the torsional levels. By analogizing the configurational basis functions centering at each well to the atomic orbitals in the molecular orbital theory, these splitting states can be treated as linear combinations of the basis functions. If a Hückel-type approximation was used,[20] i.e., only the interactions between adjacent wells were considered, a so-called tunneling matrix can be constructed (Figure 1c,d). Such tunneling matrices manifest the permutation-inversion symmetry of a nonrigid molecular system,[27] which is a key to revealing the splitting patterns. This approximation performed well in explaining the even spacing of levels and was extensively used in the early DMC[26] and low-dimensional wave-function methods.[23,28] However, it is destined to fail in describing the deviation of the torsional levels from a 1:2:1 spacing (Figure 1e).[14] High-order interactions between nonadjacent wells,[29] labeled h_2 and h_3 in this work (Figure 1a,b), must be considered since they are crucial to shift the levels and manifest the strong delocalization, as shown in Figure 1f,g,h.

Here, we use a path-integral molecular dynamics (PIMD) method[30,31] to realize a full-dimensional quantum simulation for the torsional tunneling splitting in a water trimer. A newly developed many-body water potential, which is constructed from a large data set containing hundreds of thousands of CCSD(T) points by a neural network low-error fitting, is employed for descriptions of the Born−Oppenheimer PES. High-accuracy sampling by PIMD for the density matrix elements can rigorously integrate the information of energy levels for a closed quantum system. The eigenstates are assumed to present the permutation-inversion symmetry, i.e., isomorphic to a C_6 group. The splitting levels are fitted from the density matrix elements sampled at a range of temperatures. From these simulations, the interactions h_1, h_2, and h_3 can be quantified. As a result, we reproduce the experimental value of tunneling splittings with a numerical accuracy of ∼1 cm^{-1} for both $(H_2O)_3$ and $(D_2O)_3$. The high-order nonadjacent interactions are illustrated to be crucial in this accurate simulation of the torsional levels (Figure 1h). With these, we examine the quality of the new water potential and provide a rigorous scheme to decipher the experimental spectra with unprecedented accuracy in an *ab initio* manner, which is applicable to more general systems.

THEORY

Tunneling splitting is commonly seen in the infrared and microwave spectra of gas-phase molecular systems. The coupling with other degenerate wells on IPS manifests as a splitting of vibrational levels. For the simplest symmetric double-well model,

$$\hat{H} = \begin{pmatrix} E_0 & \Delta/2 \\ \Delta/2 & E_0 \end{pmatrix} \tag{1}$$

the off-diagonal coupling term $\Delta/2$ split the ground state into $E_0 \pm \Delta/2$. When the barrier between two wells is sufficiently low, the strong coupling, also referred to as coherent tunneling of nuclei, will contribute to a noticeable splitting.

On the basis of configuration-centered Wannier functions $\{\phi(\boldsymbol{r} - \boldsymbol{r}_i) = |\boldsymbol{r}_i\rangle\}$, an effective torsional Hamiltonian for a water trimer obeying C_6 symmetry has a form

$$\hat{H} = \hat{H}_1 + \hat{H}_2 + \hat{H}_3 \tag{2}$$

with

$$\hat{H}_k = \sum_i h_k |\boldsymbol{r}_i\rangle\langle \boldsymbol{r}_{i+k}| + \text{h. c.} \tag{3}$$

If only the first nearest-neighbor (NN) term $\hat{H}_1$ is considered, as in the Hückel method, one gets a so-called tunneling matrix

https://doi.org/10.1021/jacs.2c09909
J. Am. Chem. Soc. 2022, 144, 21356−21362

and h_1:$2h_1$:h_1-spacing quartet-split levels (Figure 1e). The 2nd and 3rd NN terms (corresponding to double- and triple-flip matrix elements in ref 29), which are long-range couplings between nonadjacent wells, are significant for the quantitative interpretation of the levels' shifting observed in spectra. The eigenvalues, after subtracting the lowest level, are 0, $-h_1-3h_2-2h_3$, $-3h_1-3h_2$, and $-4h_1-2h_3$, with 1, 2, 2, and 1 degeneracy, respectively (Figure 1h, the double degeneracy comes from time-reversal symmetry). Here, we neglect the rotational-excited sublevels and their coupling to the torsional splitting and the bifurcation tunneling splittings because they are too small to be overshadowed by the sampling errors.

Density matrix element $\rho(\boldsymbol{r},\boldsymbol{r}';\beta) = \langle \boldsymbol{r}|e^{-\beta\hat{H}}|\boldsymbol{r}'\rangle$ in the low temperature limit is

$$\lim_{\beta\to\infty} \rho(\boldsymbol{r}, \boldsymbol{r}'; \beta) = \sum_{n=0}^{3}\sum_{l_n=0}^{d_n-1} \psi_{nl_n}(\boldsymbol{r})\psi_{nl_n}(\boldsymbol{r}')e^{-\beta E_n} \tag{4}$$

where β is the reverse temperature $1/k_BT$. ψ_{nl_n} is the real eigenfunction and E_n is the energy level corresponding to the nth irreducible representation. The vibrationally excited states, whose energies are much higher, can be neglected since the temperature is low.

The index l_n labels the degenerate eigenstates spanning the nth level, and the corresponding degeneracy is d_n = 1,2,2,1.

Analogous to the atomic orbitals in the molecular orbital theory, Wannier functions $\phi(\boldsymbol{r} - \boldsymbol{r}_i)$ are related to the eigenfunctions by

$$\psi_{nl_n}(\boldsymbol{r}) = \sqrt{\frac{d_n}{6}}\sum_{i=0}^{5}\cos\left(\frac{\pi n i}{3} - \frac{\pi}{2}l_n\right)\phi_i \tag{5}$$

On this orthogonal basis, the overlap integrals $S_{ij} = \langle\phi_i|\phi_j\rangle$ are exactly zero, and only a resonance (or exchange) integral $H_{ij} = \langle\phi_i|\hat{H}|\phi_j\rangle$ exists in each off-diagonal term of the Hamiltonian matrix. A sharp reduction of $\phi(\boldsymbol{r} - \boldsymbol{r}_i)$ in neighbor wells can be expected, i.e., $1 \gg \alpha_k \equiv \phi(\boldsymbol{r}_{i\pm k} - \boldsymbol{r}_i)/\phi(0)$, for $k > 0$. Then, a ratio of the density matrix elements is defined as

$$I_g(\beta) \equiv \frac{\rho(\boldsymbol{r}_0, \boldsymbol{r}_g; \beta)}{\rho(\boldsymbol{r}_0, \boldsymbol{r}_0; \beta)} = \frac{\sum_{n=0}^{3} d_n \cos\frac{\pi n g}{3}\chi_n^2 e^{-\beta E_n}}{\sum_{n=0}^{3} d_n\chi_n^2 e^{-\beta E_n}} \tag{6}$$

where $\chi_n = \sum_{i=0}^{3} d_i\alpha_i \cos(\pi n i/3)$. $I_1(\beta)$ can be accurately simulated by a combined PIMD and thermodynamic integration (PIMD + TI) method.[30] We extend the TI to the multiple-flip region to obtain $I_2(\beta)$ and $I_3(\beta)$. Finally, an easier-to-fit expression is taken, as

$$L_n \equiv -\ln\frac{1 + \sum_{g=1}^{3} I_g \cos(n\pi g/3)}{1 + 2I_1 + 2I_2 + I_3} = (\beta - \bar{\beta}_n)\,\Delta_n \tag{7}$$

with $\Delta_n = E_n - E_0$ (n = 1,2,3), and

$$\bar{\beta}_n = \frac{1}{\Delta_n}\ln\frac{1 + \sum_{i=1}^{3} d_i\alpha_i \cos(n\pi i/3)}{1 + 2\alpha_1 + 2\alpha_2 + \alpha_3} \tag{8}$$

For more details on this method, please refer to the Supporting Information.

RESULTS AND DISCUSSION

Our water potential is constructed in a many-body expansion (MBE) method.[32] The two-body term is fitted using the fundamental invariant neural network method[33] that satisfies the permutational symmetry of identical atoms, and the root-mean-square fitting error for the PES is very small as low as 0.228 meV. The database of the water dimer consists of about 220,000 *ab initio* energy points computed at the CCSD(T) level, with the Hartree−Fock and correlation energy extrapolated to the CBS limit.[34,35] The three-body term is fitted from 430,000 points of the water trimer at the CCSD(T)/AVTZ level, supplemented by an additional set of (3s,3p,2d,1f) mid-bond functions with exponents equal to (0.9, 0.3, 0.1) for s and p orbitals, (0.6, 0.2) for d, and 0.3 for f, placed at the center of mass of each trimer configuration. For both the dimer and the trimer, the counterpoise method[36] is applied to remove the basis set superposition error (BSSE). All of the trimer data are fitted in two parts by the neural network according to the second longest O−O bond length, the fitting errors of which are 0.347 meV for short-range (O−O bond less than 8 Å) and 0.027 meV for long-range (O−O bond large than 4 Å), and then the two parts are connected smoothly at 6−7 Å. The flip barrier height of our potential is 10.7 meV. This is confirmed by CCSD(T)/CBS calculation on the transition state of the water trimer, as shown in Table 1.

Table 1. Barrier Heights of Flip Motion in the Water Trimer from Different Methods

method	barrier height (meV)
our 2b-CCSD(T)/CBS + 3b-CCSD(T)/avtz	10.7
CCSD(T)/CBS	10.5[a]

[a]Ref 18.

The six degenerate configurations $\boldsymbol{r}_i$ can be easily found by structural optimizations. But their relative orientations, which are keys to being decoupled from the overall rotations, are not easy to be determined. The instanton (or kink) on a barrier, which stands for a minimum-action tunneling path,[37−39] is commonly believed to give the most reasonable orientations. We use a variable-time-step method (VTS)[40] to reduce the number of beads. The imaginary time steps are scaled to keep an even distribution of beads on Euclidean distance. The geometries of both end beads are fixed at the minimum-energy structure, but they are allowed to orientate in the action minimization process. A 200-bead instanton is optimized by the l-BFGS algorithm to ensure that the max component of the gradient is smaller than 1×10^{-5} eV/Å. Our double-flip path is constructed by splicing two single-flip instantons (from $\boldsymbol{r}_0$ to $\boldsymbol{r}_1$ and from $\boldsymbol{r}_1$ to $\boldsymbol{r}_2$) together. The first bead of the second instanton is set as the last bead of the first instanton, and both its structure and orientation are fixed in the optimization process. The triple-flip path is also spliced this way. These paths are shown in Figure S1, and they are taken as the integration paths of the TI simulations.

Compared with the semiclassical instanton method where only one tunneling barrier was considered, it might happen in the PIMD + TI simulations that other barrier regions are also sampled. A previous work treated the barriers in water clusters as isolated double-well systems and proposed a simple hyperbolic tangent function for the sampled $I_1(\beta)$.[41] From our sampling trajectories, we note that the barrier is so low on the cyclic potential of the water trimer that the PIMD simulation can easily sample outside regions of one single barrier. The linear polymer can be arbitrarily distributed between the six wells, and the beads can even wrap a large circle through the other five barriers to connect $\boldsymbol{r}_0$ and $\boldsymbol{r}_1$ (Figure 2a). As a result, eq 6 fits the sampled $I_1(\beta)$ much better

https://doi.org/10.1021/jacs.2c09909
J. Am. Chem. Soc. 2022, 144, 21356−21362

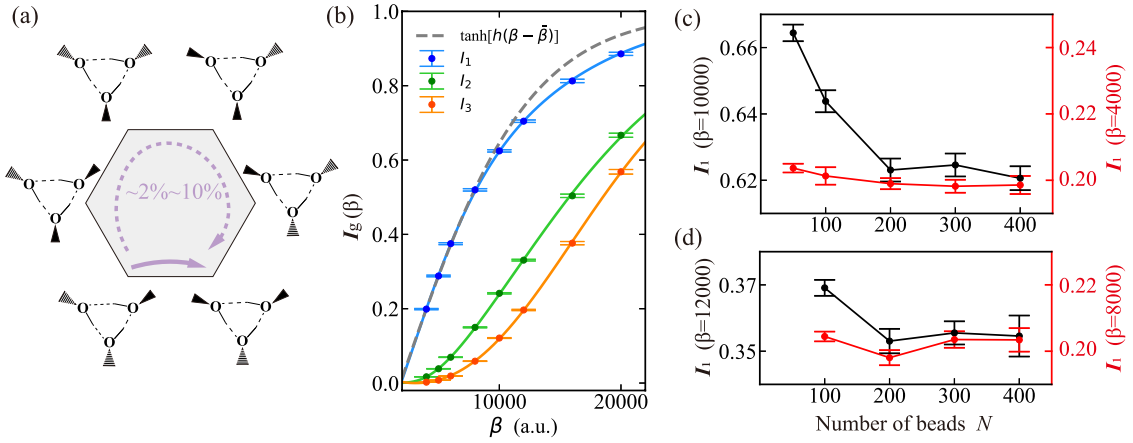

Figure 2. (a) Shows that apart from staying in the barrier region, the fixed-end linear polymer will also wrap a large circle through other barriers. The lower the temperature, the more pronounced this situation is, up to ~10% in the trajectory. (b) Shows $I_g(\beta)$ points for $(H_2O)_3$ sampled by 200 beads. The fittings using eq 6 are shown by the solid curves. The gray dotted line is fitted from the first four β points by the hyperbolic tangent function but fails to fit the other points. The convergence of $I_1(\beta)$ on a number of beads N for $(H_2O)_3$ is shown in (c) and $(D_2O)_3$ in (d).

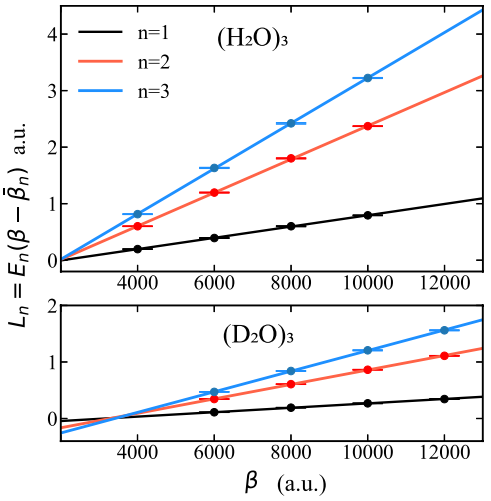

Figure 3. Sampled $L_n(\beta)$ points can be fitted well by eq 7. The ticks are error bars. Overall, 400 beads are used for $(H_2O)_3$ and 300 beads for $(D_2O)_3$.

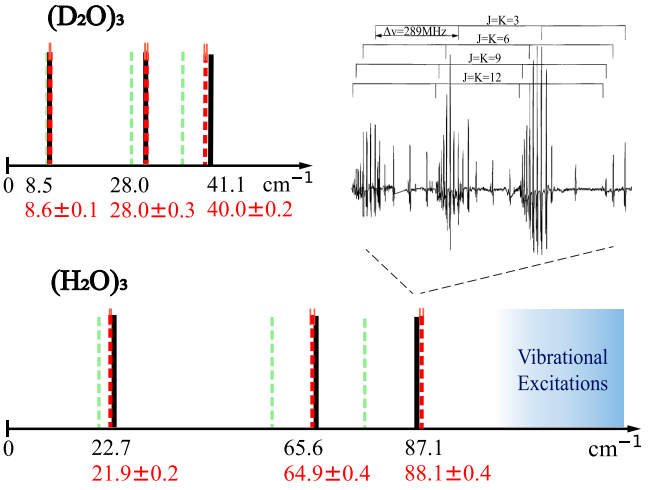

Figure 4. Red dashed lines are the calculated torsional levels of the water trimer, in comparison with experimental values[14] (black solid lines). The green dashed lines are from previous theoretical work of van der Avoird et al. by a 3-D model Hamiltonian and CC-pol + 3B potential.[25] For a comprehensive picture of the torsional bands, the inset shows part of the rotational sublevels and bifurcation splitting in the 87.1 cm^{-1} band of $(H_2O)_3$, reprinted with permission from Ref 43. Copyright 2000 American Chemical Society.

than the hyperbolic tangent functions, as shown in Figure 2b. It might also happen that an overfitting exists when six parameters (i.e., h_i and α_i, i = 1,2,3) are tuned. To cope with this problem, we simulate I_2 and I_3 and adopt eq 7. To improve the accuracy, on each flip barrier, up to 64 points for $(H_2O)_3$ and 32 points for $(D_2O)_3$ are used in the TI by the Gauss−Legendre quadrature. Each point is computed from a PIMD trajectory with at least 1×10^7 steps to ensure sufficient sampling. A Langevin thermostat especially developed for the fixed-end linear polymer[42] is used, with a scaling factor $\gamma_0 = 0.5$ for the drag coefficients. Other settings, including the mass scaling of beads and time step, have also been carefully checked. For $(H_2O)_3$, at least $1 \times 10^7 \times 3 \times 64 = 1.92 \times 10^9$ steps are sampled for one β point. Longer trajectories are run for the lower temperatures to keep the standard errors of I_g below 1%. The sampled I_gs are shown in Figure 2b.

A range of temperatures are simulated to avoid the influence of accidental sampling errors on the results and to confirm the rationality of our expression of the density matrix elements. The selected β cannot be too small, as required by the low-temperature approximation of neglecting the excited-vibrational states. It cannot be too large either, as the trajectories would be hard to converge. A suitable lower bound of β is $\sim 2\bar{\beta}$, which can be illustrated by a progressive fitting, as shown in Table S4. Then, we set a β point every 2000 a.u. The last but important factor affecting accuracy is the number of beads N used in PIMD. The convergence of I_1 on N is shown in Figure 2c,d. At higher β, more beads are needed to ensure convergence. Excellent fittings of eq 7 can be obtained for $(H_2O)_3$ and $(D_2O)_3$, as shown in Figure 3. Overall, 400 beads for $(H_2O)_3$ and 300 beads for $(H_2O)_3$ are used. The sampled $L_n(\beta)$ points from β = 4000 to 12,000 a.u. are arranged in a straight line. The standard error of each point is tiny, as shown by the almost indiscernible error bars.

With these, the split levels E_n are fitted by eq 7 in a manner of nonlinear least squares. The results are shown by the red dashed lines in Figure 4. For both $(H_2O)_3$ and $(D_2O)_3$, the torsional splitting levels coincide with experimental values. The

https://doi.org/10.1021/jacs.2c09909
J. Am. Chem. Soc. 2022, 144, 21356−21362

Table 2. Calculated Hamiltonian Matrix Elements[a]

	h_1	h_2	h_3 (cm^{-1})	α_1	α_2	α_3	$\overline{\beta}_1$	$\overline{\beta}_2$	$\overline{\beta}_3$ (10^3 a.u.)
$(H_2O)_3$	−21.8(1)	0.2(1)	−0.4(2)	−0.19	0.02	−0.01	2.04(4)	1.96(4)	1.96(2)
$(D_2O)_3$	−9.9(1)	0.6(1)	−0.2(1)	−0.15	0.03	−0.01	3.15(6)	3.29(5)	3.41(3)

[a]Numbers in parentheses are numerical errors of the last digit.

numerical errors are compressed to less than 1 cm^{-1}. The Hamiltonian matrix elements h_k and the so-called imaginary "tunneling time"[3030] $\overline{\beta}_n$ are summarized in Table 2. h_2, h_3 and α_2, α_3 are much smaller than h_1 and α_1, which is consistent with our expectation. The anomalously larger nonadjacent interactions h_2 and h_3 in $(D_2O)_3$ are correctly revealed. Notably, $-h_2$ of $(D_2O)_3$ has a negative value, which cannot be a tunneling strength or be corresponded to a tunneling frequency. Besides, the larger α_2 may be related to the larger absolute value $|h_2|$ of $(D_2O)_3$ and means a stronger nonlocality in $(D_2O)_3$. This is also contrary to intuition from conventional tunneling concepts where the lighter H should exhibit stronger tunneling. So we think it is more appropriate to call the NN terms couplings. The reproduction of the spectroscopic values is attributed to a combined effort of this full-dimensional theory and the water potential energy surface. Previous works by a low-dimensional model gave a smaller splitting size, suffering from an oversimplification of the cooperative motion of nuclei, which would lead to an overestimated barrier height by up to 10%.[25] Their result from a 3-D model Hamiltonian and the cc-pol + 3B water potential is shown by the green dashed lines in Figure 4. Our result indicates that in a quantitative simulation, the cooperative motions of the oxygen and bonded hydrogen are also important. Our method shall apply without hindrance to the similar flip tunneling splitting in a water pentamer where the cooperative motions of oxygen are more pronounced.

CONCLUSIONS

We provide a recipe for full-dimensional quantum simulations of the torsional tunneling splitting in a water trimer. Our *ab initio* simulations show that the splitting sizes are comparable to experiments with accuracy up to ∼1 cm^{-1}. We numerically demonstrate the limitation of the Hückel model and show that the high-order NN terms between nonadjacent wells of the configurational space are important for the interpretation of the splitting energy levels' shifting. This effect might be present in multifold tunneling splittings in other water clusters and molecular systems as well. With this endeavor, we examined the quality of our new water potential and provided a rigorous scheme for deciphering the experimental spectra with unprecedented high accuracy, which is applicable to more general systems. This methodology presents a new route toward designing systematically improvable water potentials, with highly accurate VRT experimental spectra being able to be used as calibrators.

ASSOCIATED CONTENT

Supporting Information

The Supporting Information is available free of charge at https://pubs.acs.org/doi/10.1021/jacs.2c09909.

PIMD+TI method, instantons as paths of TI, simulation data of the ratio of density matrix elements $I_g(\beta)$ and fitting results, and details on constructing the water potential (PDF)

AUTHOR INFORMATION

Corresponding Authors

Dong H. Zhang − *State Key Laboratory of Molecular Reaction Dynamics, Dalian Institute of Chemical Physics, Chinese Academy of Sciences, Dalian 116023, People's Republic of China;* orcid.org/0000-0001-9426-8822; Email: zhangdh@dicp.ac.cn

Xin-Zheng Li − *State Key Laboratory for Artificial Microstructure and Mesoscopic Physics, Frontier Science Center for Nano-optoelectronics and School of Physics, Peking University, Beijing 100871, People's Republic of China; Interdisciplinary Institute of Light-Element Quantum Materials, Research Center for Light-Element Advanced Materials, and Collaborative Innovation Center of Quantum Materials, Peking University, Beijing 100871, People's Republic of China; Peking University Yangtze Delta Institute of Optoelectronics, Nantong, Jiangsu 226010, People's Republic of China;* orcid.org/0000-0003-0316-4257; Email: xzli@pku.edu.cn

Authors

Yu-Cheng Zhu − *State Key Laboratory for Artificial Microstructure and Mesoscopic Physics, Frontier Science Center for Nano-optoelectronics and School of Physics, Peking University, Beijing 100871, People's Republic of China; Interdisciplinary Institute of Light-Element Quantum Materials, Research Center for Light-Element Advanced Materials, and Collaborative Innovation Center of Quantum Materials, Peking University, Beijing 100871, People's Republic of China;* orcid.org/0000-0003-2255-025X

Shuo Yang − *State Key Laboratory of Molecular Reaction Dynamics, Dalian Institute of Chemical Physics, Chinese Academy of Sciences, Dalian 116023, People's Republic of China; University of Chinese Academy of Sciences, Beijing 100871, People's Republic of China*

Jia-Xi Zeng − *State Key Laboratory for Artificial Microstructure and Mesoscopic Physics, Frontier Science Center for Nano-optoelectronics and School of Physics, Peking University, Beijing 100871, People's Republic of China; Interdisciplinary Institute of Light-Element Quantum Materials, Research Center for Light-Element Advanced Materials, and Collaborative Innovation Center of Quantum Materials, Peking University, Beijing 100871, People's Republic of China*

Wei Fang − *State Key Laboratory of Molecular Reaction Dynamics, Dalian Institute of Chemical Physics, Chinese Academy of Sciences, Dalian 116023, People's Republic of China; Department of Chemistry, Fudan University, Shanghai 200438, People's Republic of China;* orcid.org/0000-0001-9584-8466

Ling Jiang − *State Key Laboratory of Molecular Reaction Dynamics, Dalian Institute of Chemical Physics, Chinese Academy of Sciences, Dalian 116023, People's Republic of China;* orcid.org/0000-0002-8485-8893

Complete contact information is available at:

https://pubs.acs.org/10.1021/jacs.2c09909

Author Contributions

∇

Y.-C.Z. and S.Y.Contributed equally to this work.

Notes

The authors declare no competing financial interest.

■ ACKNOWLEDGMENTS

The authors are supported by the National Science Foundation of China under Grant Nos. 12234001, 11934003, and 22288201; the National Basic Research Programs of China under Grand No. 2021YFA1400503; the Beijing Natural Science Foundation under Grant No. Z200004; and the Strategic Priority Research Program of the Chinese Academy of Sciences under Grant No. XDB33010400. The computational resources were provided by the supercomputer center at Peking University, China.

■ REFERENCES

(1) Bukowski, R.; Szalewicz, K.; Groenenboom, G. C.; Van der Avoird, A. Predictions of the properties of water from first principles. *Science* **2007**, *315*, 1249.

(2) Fellers, R. S.; Leforestier, C.; Braly, L. B.; Brown, M. G.; Saykally, R. J. Spectroscopic Determination of the Water Pair Potential. *Science* **1999**, *284*, 945.

(3) Paesani, F. Getting the Right Answers for the Right Reasons: Toward Predictive Molecular Simulations of Water with Many-Body Potential Energy Functions. *Acc. Chem. Res.* **2016**, *49*, 1844.

(4) Babin, V.; Medders, G. R.; Paesani, F. Toward a Universal Water Model: First Principles Simulations from the Dimer to the Liquid Phase. *J. Phys. Chem. Lett.* **2012**, *3*, 3765.

(5) Babin, V.; Leforestier, C.; Paesani, F. Development of a "First Principles" Water Potential with Flexible Monomers: Dimer Potential Energy Surface, VRT Spectrum, and Second Virial Coefficient. *J. Chem. Theory Comput.* **2013**, *9*, 5395.

(6) Wang, Y.; Huang, X.; Shepler, B. C.; Braams, B. J.; Bowman, J. M. Flexible, ab initio potential, and dipole moment surfaces for water. I. Tests and applications for clusters up to the 22-mer. *J. Chem. Phys.* **2011**, *134*, No. 094509.

(7) Keutsch, F. N.; Saykally, R. J. Water clusters: Untangling the mysteries of the liquid, one molecule at a time. *Proc. Natl. Acad. Sci. U.S.A.* **2001**, *98*, No. 10533.

(8) Pugliano, N.; Saykally, R. Measurement of quantum tunneling between chiral isomers of the cyclic water trimer. *Science* **1992**, *257*, 1937.

(9) Cruzan, J. D.; Braly, L.; Liu, K.; Brown, M.; Loeser, J.; Saykally, R. Quantifying hydrogen bond cooperativity in water: VRT spectroscopy of the water tetramer. *Science* **1996**, *271*, 59.

(10) Liu, K.; Brown, M. G.; Cruzan, J. D.; Saykally, R. J. Vibration-Rotation Tunneling Spectra of the Water Pentamer: Structure and Dynamics. *Science* **1996**, *271*, 62.

(11) Pérez, C.; Muckle, M. T.; Zaleski, D. P.; Seifert, N. A.; Temelso, B.; Shields, G. C.; Kisiel, Z.; Pate, B. H. Structures of Cage, Prism, and Book Isomers of Water Hexamer from Broadband Rotational Spectroscopy. *Science* **2012**, *336*, 897.

(12) Richardson, J. O.; Pérez, C.; Lobsiger, S.; Reid, A. A.; Temelso, B.; Shields, G. C.; Kisiel, Z.; Wales, D. J.; Pate, B. H.; Althorpe, S. C. Concerted hydrogen-bond breaking by quantum tunneling in the water hexamer prism. *Science* **2016**, *351*, 1310.

(13) Zwart, E.; ter Meulen, J.; Meerts, W. L.; Coudert, L. The submillimeter rotation tunneling spectrum of the water dimer. *J. Mol. Spectrosc.* **1991**, *147*, 27.

(14) Keutsch, F. N.; Cruzan, J. D.; Saykally, R. J. The Water Trimer. *Chem. Rev.* **2003**, *103*, 2533.

(15) Stone, A. J. Water from First Principles. *Science* **2007**, *315*, 1228.

(16) Schwan, R.; Qu, C.; Mani, D.; Pal, N.; Schwaab, G.; Bowman, J. M.; Tschumper, G. S.; Havenith, M. Observation of the Low-Frequency Spectrum of the Water Trimer as a Sensitive Test of the Water-Trimer Potential and the Dipole-Moment Surface. *Angew. Chem., Int. Ed.* **2020**, *59*, No. 11399.

(17) Wang, X.-G.; Carrington, T., Jr Using monomer vibrational wavefunctions to compute numerically exact (12D) rovibrational levels of water dimer. *J. Chem. Phys.* **2018**, *148*, No. 074108.

(18) Anderson, J. A.; Crager, K.; Fedoroff, L.; Tschumper, G. S. Anchoring the potential energy surface of the cyclic water trimer. *J. Chem. Phys.* **2004**, *121*, No. 11023.

(19) Keutsch, F. N.; Brown, M. G.; Petersen, P. B.; Saykally, R. J.; Geleijns, M.; van der Avoird, A. Terahertz vibration-rotation-tunneling spectroscopy of water clusters in the translational band region of liquid water. *J. Chem. Phys.* **2001**, *114*, 3994.

(20) Wales, D. J. Theoretical study of water trimer. *J. Am. Chem. Soc.* **1993**, *115*, No. 11180.

(21) Walsh, T. R.; Wales, D. J. Rearrangements of the water trimer. *J. Chem. Soc., Faraday Trans.* **1996**, *92*, 2505.

(22) Schütz, M.; Bürgi, T.; Leutwyler, S.; Bürgi, H. B. Fluxionality and low-lying transition structures of the water trimer. *J. Chem. Phys.* **1993**, *99*, 5228.

(23) van der Avoird, A.; Olthof, E. H. T.; Wormer, P. E. S. Tunneling dynamics, symmetry, and far-infrared spectrum of the rotating water trimer. I. Hamiltonian and qualitative model. *J. Chem. Phys.* **1996**, *105*, 8034.

(24) Sabo, D.; Bačić, Z.; Graf, S.; Leutwyler, S. Rotational constants of all H/D substituted water trimers: Coupling of intermolecular torsional and symmetric stretching modes. *J. Chem. Phys.* **1999**, *110*, 5745.

(25) van der Avoird, A.; Szalewicz, K. Water trimer torsional spectrum from accurate ab initio and semiempirical potentials. *J. Chem. Phys.* **2008**, *128*, No. 014302.

(26) Gregory, J. K.; Clary, D. C. Calculations of the tunneling splittings in water dimer and trimer using diffusion Monte Carlo. *J. Chem. Phys.* **1995**, *102*, 7817.

(27) Longuet-Higgins, H. The symmetry groups of non-rigid molecules. *Mol. Phys.* **1963**, *6*, 445.

(28) Olthof, E. H. T.; van der Avoird, A.; Wormer, P. E. S.; Liu, K.; Saykally, R. J. Tunneling dynamics, symmetry, and far-infrared spectrum of the rotating water trimer. II. Calculations and experiments. *J. Chem. Phys.* **1996**, *105*, 8051.

(29) Keutsch, F. N.; Saykally, R. J.; Wales, D. J. Bifurcation tunneling dynamics in the water trimer. *J. Chem. Phys.* **2002**, *117*, 8823.

(30) Mátyus, E.; Wales, D. J.; Althorpe, S. C. Quantum tunneling splittings from path-integral molecular dynamics. *J. Chem. Phys.* **2016**, *144*, No. 114108.

(31) Mátyus, E.; Althorpe, S. C. Calculating splittings between energy levels of different symmetry using path-integral methods. *J. Chem. Phys.* **2016**, *144*, No. 114109.

(32) Hankins, D.; Moskowitz, J.; Stillinger, F. Water molecule interactions. *J. Chem. Phys.* **1970**, *53*, 4544.

(33) Derksen, H.; Kemper, G.*Computational Invariant Theory*; Springer; 2015, Chapter 3.

(34) Halkier, A.; Klopper, W.; Helgaker, T.; Jørgensen, P.; Taylor, P. R. Basis set convergence of the interaction energy of hydrogen-bonded complexes. *J. Chem. Phys.* **1999**, *111*, 9157.

(35) Halkier, A.; Helgaker, T.; Jørgensen, P.; Klopper, W.; Olsen, J. Basis-set convergence of the energy in molecular Hartree-Fock calculations. *Chem. Phys. Lett.* **1999**, *302*, 437.

(36) Boys, S. F.; Bernardi, F. The calculation of small molecular interactions by the differences of separate total energies. Some procedures with reduced errors. *Mol. Phys.* **1970**, *19*, 553.

(37) Richardson, J. O.; Althorpe, S. C.; Wales, D. J. Instanton calculations of tunneling splittings for water dimer and trimer. *J. Chem. Phys.* **2011**, *135*, No. 124109.

(38) Fang, W.; Chen, J.; Pedevilla, P.; Li, X.-Z.; Richardson, J. O.; Michaelides, A. Origins of fast diffusion of water dimers on surfaces. *Nat. Commun.* **2020**, *11*, No. 1689.

(39) Fang, W.; Richardson, J. O.; Chen, J.; Li, X.-Z.; Michaelides, A. Simultaneous Deep Tunneling and Classical Hopping for Hydrogen Diffusion on Metals. *Phys. Rev. Lett.* **2017**, *119*, No. 126001.
(40) Cvitaš, M. T.; Althorpe, S. C. Locating Instantons in Calculations of Tunneling Splittings: The Test Case of Malonaldehyde. *J. Chem. Theory Comput.* **2016**, *12*, 787.
(41) Vaillant, C. L.; Wales, D. J.; Althorpe, S. C. Tunneling Splittings in Water Clusters from Path Integral Molecular Dynamics. *J. Phys. Chem. Lett.* **2019**, *10*, 7300.
(42) Vaillant, C. L.; Wales, D.; Althorpe, S. Tunneling splittings from path-integral molecular dynamics using a Langevin thermostat. *J. Chem. Phys.* **2018**, *148*, No. 234102.
(43) Wormer, P. E. S.; van der Avoird, A. Intermolecular Potentials, Internal Motions, and Spectra of van der Waals and Hydrogen-Bonded Complexes. *Chem. Rev.* **2000**, *100*, 4109.

https://doi.org/10.1021/jacs.2c09909
J. Am. Chem. Soc. 2022, 144, 21356−21362